Lab on a Chip

PAPER

Cite this: *Lab Chip*, 2022, **22**, 4693

A microfluidic fully paper-based analytical device integrated with loop-mediated isothermal amplification and nano-biosensors for rapid, sensitive, and specific quantitative detection of infectious diseases

Hamed Tavakoli,†[a] Elisabeth Hirth,†[ab] Man Luo,[a] Sanjay Sharma Timilsina,[a] Maowei Dou,[a] Delfina C. Dominguez[c] and XiuJun Li *[ade]

Received 6th September 2022,
Accepted 2nd November 2022

DOI: 10.1039/d2lc00834c

rsc.li/loc

Bacterial meningitis, an infection of the membranes (meninges) and cerebrospinal fluid (CSF) surrounding the brain and spinal cord, is one of the major causes of death and disability worldwide. Higher case-fatality rates and short survival times have been reported in developing countries. Hence, a quick, straightforward, and low-cost approach is in great demand for the diagnosis of meningitis. In this research, a microfluidic fully paper-based analytical device (μFPAD) integrated with loop-mediated isothermal amplification (LAMP) and ssDNA-functionalized graphene oxide (GO) nano-biosensors was developed for the first time for a simple, rapid, low-cost, and quantitative detection of the main meningitis-causing bacteria, *Neisseria meningitidis* (*N. meningitidis*). The results can be successfully read within 1 hour with the limit of detection (LOD) of 6 DNA copies per detection zone. This paper device also offers versatile functions by providing a qualitative diagnostic analysis (*i.e.*, a yes or no answer), confirmatory testing, and quantitative analysis. These features make the presented μFPAD capable of a simple, highly sensitive, and specific diagnosis of *N. meningitis*. Furthermore, this microfluidic approach has great potential in the rapid detection of a wide variety of different other pathogens in low-resource settings.

1. Introduction

Meningitis is a life-threatening inflammation of the meninges of the human brain and cerebrospinal fluid (CSF) of the human central nervous system. It can be caused by viruses, fungi, bacteria, or other nonpathogenic agents like amoeba and endoparasites. Although viral, fungal, and other nonpathogenic forms of meningitis are often mild and rare, bacterial meningitis appears very common and results in brain damage, hearing loss, learning disability, and death in more severe cases.[1–3] Bacterial meningitis is one of the ten leading causes of death due to infectious diseases worldwide. About 10% of the patients die within 24–48 h of the onset of symptoms and long-term neurological sequelae occur in 10–20% of survivors.[4] The bacterial meningitis is mainly caused by *Neisseria meningitidis* bacterium, also known as *meningococcal meningitis*, which is the major cause of fatal meningitis in humans and spreads rapidly among people through coughing, sneezing, or close contact.[3] Moreover, the symptoms of meningitis are similar to that of the common flu, which makes meningitis diagnosis difficult based on clinical symptoms.[5] Hence, a simple, quick, and highly sensitive methodology is essential to the immediate and early diagnosis of meningitis.

Traditional methods for diagnosis of meningitis involve the culture of bacteria, latex agglutination test, and coagglutination assay.[6,7] While culture takes a long time, the other two tests include a series of enzymatic reactions, which may lead to uncertain results.[3,8] Gram staining and other biochemical methods for diagnosis of meningitis are preliminary methods of differentiating Gram-negative from Gram-positive bacteria or one group of bacteria from others. These tests can be misled patients with prior antibiotic treatment.[9,10] New molecular techniques such as quantitative real-time polymerase chain reaction (qPCR)[11–13] and loop-

[a] *Department of Chemistry and Biochemistry, University of Texas at El Paso, El Paso, Texas, 79968, USA. E-mail: xli4@utep.edu; Fax: +1(915)747 5748; Tel: +1(915)747 8967*
[b] *Department of Chemistry, University of Aalen, Beethovenstraße 1, 73430 Aalen, Germany*
[c] *College of Health Sciences, University of Texas at El Paso, El Paso, TX, USA*
[d] *Border Biomedical Research Center, Biomedical Engineering, University of Texas at El Paso, El Paso, 79968, USA*
[e] *Environmental Science and Engineering, University of Texas at El Paso, El Paso, 79968, USA*
† Denotes equal contributions.

mediated isothermal amplification (LAMP)[14,15] have been used to overcome these problems and provide faster detection of bacterial meningitis. Although qPCR is a valuable method for detecting bacterial meningitis,[16] this method requires specialized personnel and equipment and is consequently costly.[17] LAMP has been developed as a new method to amplify DNA with high specificity, efficiency, and rapidity under isothermal conditions. There are several reports on LAMP amplification techniques for the detection of bacterial meningitis.[18–20] However, like qPCR, specialized equipment and laborious procedure are required for conventional LAMP, which limits its broad application in the field or the low-resource settings.[21]

Microfluidic lab-on-a-chip (LOC) offers a unique opportunity for highly efficient human health diagnostics[22–29] because of various advantages, including miniaturization, integration, automation, and low sample consumption. The LOC technology provides high potential for the point of care (POC) diagnosis of a wide range of diseases in low-resource settings. Fabrication methods and cost of microfluidic platforms, assay, and detection procedures can be significantly affected by the substrates used to fabricate a microfluidic device such as glass,[30] polydimethylsiloxane (PDMS),[21,31] and paper.[32–34] Paper is one of the most common low-cost materials for microfluidic device fabrication that is simple, easy to fabricate, and does not need complex surface treatment procedures to immobilize biosensors on a microfluidic platform.[35] Hydrophobic barriers can be patterned on paper to create microfluidic channels without the need for cleanroom facilities.[36] The porous chromatography paper also presents a simple 3D substrate for reagent storage and reactions.[37] In addition, The cellulose paper is biodegradable, and fluids can be transported *via* the capillary effect through the paper without using external pneumatic pumps or electric power.[35] These properties make paper-based microfluidic devices ideal for low-cost POC detection of infectious diseases.

The combination of LAMP with microfluidic technology miniaturizes conventional LAMP detection systems and facilitates the realization of POC pathogen detection in different desired healthcare settings. Unlike PCR, on-chip LAMP usually does not need complicated microfabrication of heaters and temperature sensors on a microfluidic chip,[18,38] making it ideal for POC pathogen detection in low-resource settings. Recently, porous materials such as microscale hydrogel (microgel) and paper integrated with LAMP reactions presented a high potential for nucleic acid detection because of their 3D porous network structures and excellent biocompatibility.[39,40] In addition, polymer-based,[41–43] polymer/paper hybrid, and other paper hybrid microfluidic devices[44–47] integrated with the LAMP amplification method have been developed for rapid detection of pathogens. However, it is challenging to integrate LAMP on a fully paper-based microfluidic device due to reagent evaporation associated with the LAMP amplification process at approximately 60–65 °C for about one hour.[48–51] Thus, most paper-based LAMP relied on the combination with other chip substrates such as glass to achieve on-chip LAMP on paper-based devices.[48] For instance, Yoon and co-workers developed a paper-based microfluidic device integrated with LAMP for the qualitative detection of the Zika virus.[48] But the device still relied on assistance from two glass plates, which was essentially equivalent to a paper/glass hybrid device,[52–54] and required multiple separate procedures that were not integrated with a single device. Moreover, some paper-based devices integrated with LAMP were reported for the detection of methicillin-resistant *Staphylococcus aureus* (MRSA).[51,55] The presented devices were not, accurately speaking, microfluidic devices because they contained circular holes without any microfluidic channels. Therefore, there are no fully paper-based integrated microfluidic LAMP devices reported yet. In addition, although amplification results can be virtually detected by using organic fluorescence dyes such as calcein and SYBR Green by the naked eye, they have some drawbacks such as limited quantitative analysis, low specificity, and a high rate of false-positive results.[18,21,22]

Herein, we developed a simple, novel, and low-cost microfluidic fully paper-based analytical device (μFPAD) integrated with LAMP reaction for the rapid and sensitive quantitative detection of the main meningitis-causing bacterium, *N. meningitidis*. Due to the unique optical, electronic, and mechanical properties of nanomaterials for quantitative analysis nucleic acids analysis with high detection sensitivity,[37,56,57] we also integrated single-strand DNA (ssDNA)-functionalized graphene oxide (GO) nano-biosensors on the μFPAD for specific and quantitative diagnosis of meningitis, applying a simple "turn on" approach based on the fluorescence quenching and recovery property of graphene oxide while adsorbing and desorbing Cy3-labeled ssDNAs.[37,56] Our device is fully made out of chip substrate paper, so it is economical and easy to fabricate and incinerate. To the best of our knowledge, this is the first fully paper-based microfluidic chip integrated with LAMP amplification and nano-biosensors for the rapid quantitative diagnosis of infectious diseases. In addition, without complicated surface modification procedures for ssDNA probe immobilization, the ssDNA-functionalized GO biosensor is integrated on the μFPAD for specific and quantitative detection of *N. meningitides*, while paper acts as a simple 3D storage substrate for the ssDNA-functionalized GO nano-biosensor. The μFPAD is not only capable of qualitative analysis (*i.e.*, giving a yes or no answer) but also quantitative detection, addressing a major problem in LAMP quantitation. The results can be successfully read within 1 hour with a limit of detection (LOD) of 6 DNA copies, comparable to conventional qPCR. Furthermore, the demonstrated multiplexed detection of *N. meningitides* and *S. pneumoniae* with high specificity indicates a great potential of the μFPAD for simultaneous quantitation of various infectious diseases.

2. Experimental section

2.1. Chemicals and materials

LAMP kits were purchased from Eiken Co. Ltd., Japan. The LAMP reaction mixture was prepared by following the manufacturer's protocol. Table 1 shows the LAMP primers and ssDNA probe obtained from Integrated DNA Technologies (Coralville, IA) for the target DNA sequences of the genes of *N. meningitidis ctrA* and *S. pneumoniae lytA*. All the ssDNA probes were labeled with Cy3 at the 5′ end. GO was obtained from Graphene Laboratories (Calverton, NY). Whatman chromatography paper and all other mentioned chemicals and solvents were obtained from Sigma (St. Louis, MO) and used without further purification unless noted otherwise. Unless otherwise stated, all solutions were prepared with ultrapure Milli-Q water (18.2 MV cm) from a Millipore Milli-Q system (Bedford, MA).

2.2. Microorganism culture and DNA preparation

N. meningitidis (ATCC 13098) and *S. pneumoniae* (ATCC 49619) were purchased from American Type Culture Collection (ATCC, Rockville, MD). Chocolate II agar plates (BD, Sparks, MD) and TSA II agar plates supplemented with 5% sheep blood (BD, Sparks, MD) were used to grow *N. meningitidis* and *S. pneumoniae*, respectively. All the microorganisms were incubated at 37 °C for 48 h in an aerobic environment with 5% CO_2.

The Qiagen DNA Mini Kit was used to extract DNA following a slightly modified protocol from the manufacturer to test the feasibility of the on-chip LAMP detection of *N. meningitidis*. Briefly, harvested bacterial cells in 5 mL sterile saline (maximum 2×10^9 cells were adjusted to 0.5 turbidity McFarland standard) from a bacterial culture plate and then centrifuged at 5000 × *g* (or 7500 rpm) for 10 min. After discarding the supernatant, the bacterial pellet was collected for the remaining DNA preparation procedures following the manufacturer's protocol. The concentration of the template DNA and the LAMP products were determined using Nanodrop (Nanodrop 1000, Thermo Scientific, MA). Alternatively, bacteria cells were lysed using a centrifuge-free method that we developed recently.[58]

2.3. Layout and fabrication of the μFPAD

The microfluidic device consists of five layers, as illustrated in Fig. 1. The top layer is a paper layer, including 3 detection zones and 3 hydrophilic channels for LAMP product delivery. The second layer is a parafilm layer to separate the LAMP zone from the top layer. The third and fourth layers are two paper layers forming some cylindrically shaped space as a LAMP zone (diameter 5 mm) for the LAMP reaction. To prevent potential reagents from spreading into the space between the two middle paper layers, the outer walls of the LAMP zone were sealed with super glue to generate a hydrophobic border. The bottom layer is packing tape for structure support.

To generate the hydrophilic channels and detection zones on the top paper layer, a piece of Whatman #4 chromatography paper was treated using SU-8. A photomask was designed and printed on a transparency slide with a standard printer. The photomask was aligned with the hydrophilic SU-8 treated chromatography paper and exposed to UV radiation under a UV exposure machine (intensity 100%, 20 seconds). To assemble different layers, a layer of commercially available double-sided carpet tape was used between both the paper layers and the Parafilm.

Before assembly of the biochip, the prepared LAMP mixture (without samples) based on the manufacturer's protocol was pre-loaded to the LAMP zone. 1 μL of 0.03 mg ml^{-1} GO and 1 μL of 1 μM Cy-3 labeled ssDNA probe were preloaded to the detection zones of the top paper layer. After sealing the top layer with tape, the biochip became a ready-to-use device.

2.4. On-chip LAMP procedure

An *N. meningitidis* sample was introduced to the biochip from the bottom packing tape layer to the LAMP zone using a

Table 1 Sequence information of LAMP primers and ssDNA probes for *N. meningitidis* and *S. pneumoniae*

N. meningitidis ctrA LAMP primer sequences and the probe sequences		
LAMP primer	Sequences (5′–3′)	No. of bases
FIP	CAAACACACCACGCGCATCAGATCTGAAGCCATTGGCCGTA	41
BIP	TGTTCCGCTATACGCCATTGGTACTGCCATAACCTTGAGCAA	42
F3	AGC(C/T)AGAGGCTTATCGCTT	19
B3	ATACCGTTGGAATCTCTGCC	20
FL	CGATCTTGCAAACCGCCC	18
BL	GCAGAACGTCAGGATAAATGGA	22
Probe	Cy3-AACCTTGAGCAATCCATTTATCCTGACGTTCT	32
S. pneumoniae lytA LAMP primer sequences and the probe sequences		
LAMP primer	Sequences (5′–3′)	No. of bases
FIP	CCGCCAGTGATAATCCGCTTCACACTCAACTGGGAATCCGC	41
BIP	TCTCGCACATTGTTGGGAACGGCCAGGCACCATTATCAACAGG	43
F3	GCGTGCAACCATATAGGCAA	20
B3	AGCATTCCAACCGCC	15
BL	TGCATCATGCAGGTAGGA	18
Probe	Cy3-GCGGATTCCCAGTTGAGTGTGCGTGTAC	28

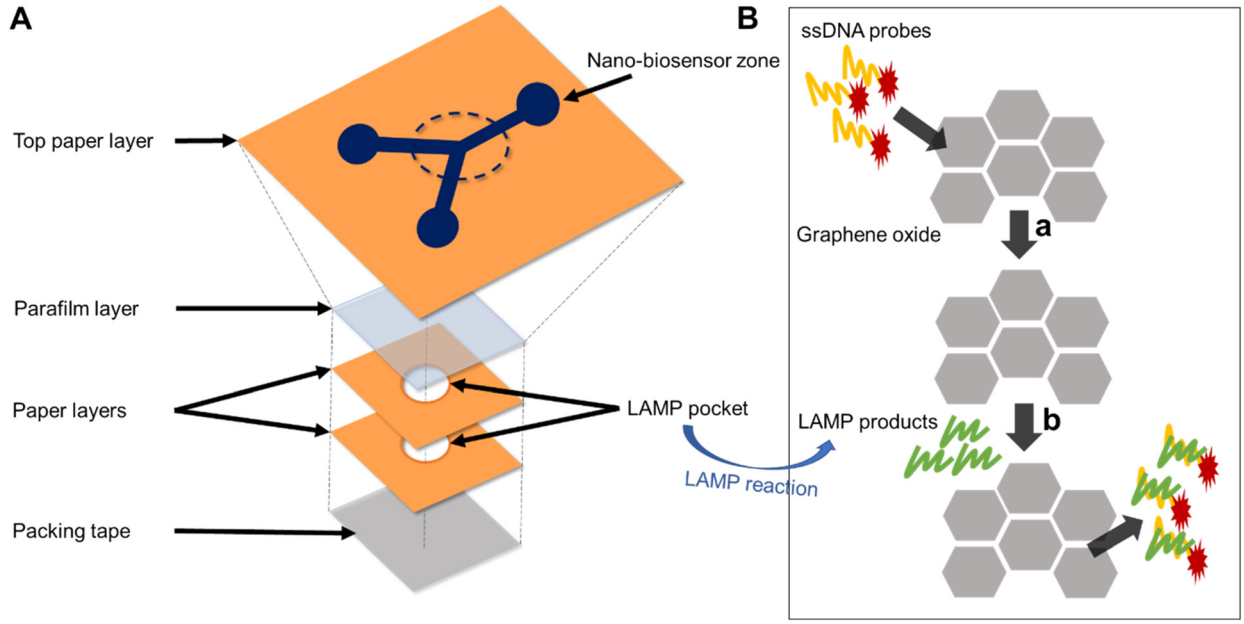

Fig. 1 Schematic of the μFPAD integrated with LAMP and ssDNA-functionalized GO nano-biosensors to detect *N. meningitidis*. (A) 3D illustration of the chip layout. (B) Detection principle based on the interaction among the GO, the ssDNA probe, and the LAMP products.

micro syringe. After the generated hole was sealed with tape, the microfluidic device was placed on a battery-powered portable heater at 63 °C for 1 h for LAMP reactions, and then the LAMP reactions were terminated at 95 °C for 2 min.

After the LAMP reaction, an innovative poking-flipping actuation method was developed to transfer LAMP products to nanosensor zones. Briefly, a thumbtack was used to make a small hole into the packing tape and the Parafilm from the bottom of the chip. By flipping the chip over, the LAMP products flowed into the hydrophilic channels on the top paper layer and were then distributed to different nano-biosensor detection zones to hybridize with the Cy3-labeled ssDNA probes. The device was incubated for 20 min at room temperature and then was scanned by a Nikon fluorescence microscope (Melville, NY) equipped with a Cy3 optical filter (E_x = 550 nm; E_m = 570 nm) to measure the fluorescence intensity. LAMP products were also analyzed using gel electrophoresis (Sub-Cell GT, Bio-Rad, CA). For gel electrophoresis, 90 V was applied for 1 h in 1.5% agarose gel to resolve the amplified products.

3. Results and discussion

3.1. A fully paper-based microfluidic device for on-chip LAMP reaction

Paper is an economical material for easily fabricating microfluidic chips, which does not need a complicated surface modification procedure for nano-sensor integration on the chip. In this work, the presented device is a fully paper-based microfluidic device including one top paper layer and two middle paper layers (note, by convention, glue and tape are not considered as chip substrates like silicon, glass, PDMS, poly(methyl methacrylate) (PMMA), polycarbonate (PC), and so on). Different from other on-chip LAMP work,[48] two dedicated middle paper layers were used to form the LAMP zone in order to increase the volume of the cylindrical LAMP reaction space to hold more LAMP mixtures. Parafilm and packing tape layers were used to seal the top and the bottom of the LAMP zone, respectively. All layers were assembled using double-sided carpet tape. To prevent LAMP reagents from spreading into the possible gap between paper layers, which would cause contamination and false-positive results, the outer walls of the LAMP zone were coated with hydrophobic commercially available super glue, ensuring the watertight of the LAMP zone. Parafilm, tape, and super glue were chosen due to their hydrophobicity, transparency, availability, cost-effectiveness, and stability.

To achieve high sensitivity detection, LAMP was integrated on the fully paper-based microfluidic device. The LAMP method is a simple, rapid, sensitive, and cost-effective DNA amplification method that allows isothermal DNA amplification at a constant temperature compared to PCR.[38] Before the biochip assembly, the prepared LAMP mixture (without samples) and ssDNA-functionalized GO were preloaded to the LAMP zone and the detection zones in the top paper layer, respectively, forming a ready-to-use device. This ready-to-use device only needed sample injection by users during testing, thus minimizing the operation procedures. As shown in Fig. 2B, a micro syringe was used to inject the *N. meningitidis* DNA sample from the bottom of the chip to the LAMP zone and the created hole was sealed using a small piece of tape. Then, the μFPAD was taken to a battery-powered portable heater for LAMP reactions at 63 °C for 1 h.

To achieve quantitative detection, Cy3-ssDNA-functionalized GO nano-biosensors were also integrated into the μFPAD. After the adsorption of fluorescent-labeled ssDNA

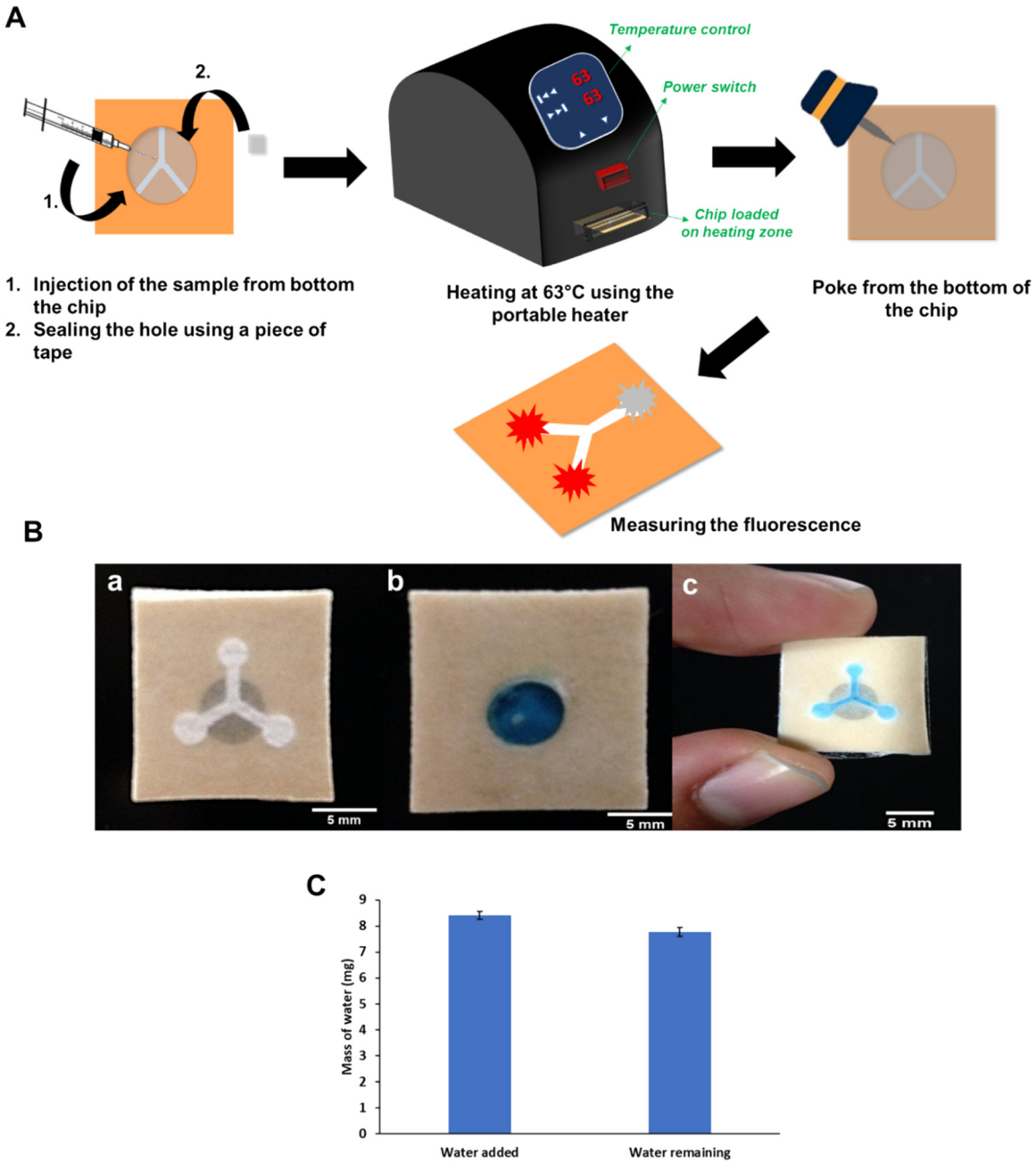

Fig. 2 (A) Schematic illustration of the assay procedure using μFPAD. (B) Reagent delivery test of μFPAD. (a) Top view of μFPAD before poking; (b) bottom view of μFPAD before poking, with the LAMP reaction zone in the device filled with a blue food dye; (c) a photograph of μFPAD after poking and delivering the blue food dye into the channels and the detection zones (top view). (C) Testing reagent loss due to evaporation after 1 hour of heating at 63 °C (n = 3).

probes on the GO surface, the fluorescence is quenched (fluorescence 'OFF') before the sample injection because GO has an extraordinary distance-dependent fluorescence quenching property.[59,60] During testing, a thumbtack was used to make a small hole into the packing tape and the Parafilm layers from the bottom of the chip. Then, by flipping the chip over, the isothermally amplified DNA targets in the LAMP zone were delivered to the nano-biosensor detection zones due to gravity (Fig. 2A). The ssDNA probe forms a duplex after a specific binding with the target. The binding of the probe and target causes a conformational change of the probe so that it becomes rigid,[61,62] leading to a lower affinity of the duplex with GO and the subsequent spontaneous liberation of the ssDNA probe from the GO surface. As illustrated in Fig. 1B, the distance between the fluorescence dye and GO is too far to quench the fluorescence efficiently after the release of the probe from the GO surface. It reverts the quenching effect (fluorescence 'ON'). No fluorescence is observed when there is no target.[37] In addition to the quantitation of DNA targets, a very high

specificity was achieved using the μFPAD because specific LAMP primers and specific DNA capture probes acted as double checkpoints. As shown above, pre-loaded LAMP and sensor reagents, LAMP reactions, smart pocking-flipping actuation, and nanosensor quantitation were all integrated in a single fully paper-based device, which minimized DNA contamination and separate user operations, enhanced portability and functionality, while maintaining high biosafety levels to users.

The LAMP product needs to be delivered into the detection zones for the on-chip LAMP detection. To test and illustrate the reagent delivery process, the LAMP zone was filled with blue food dye, followed by the same LAMP product delivery procedure mentioned above. Fig. 2B(a and b) show the top and the bottom views of the μFPAD filled with the blue food dye before actuating the Parafilm valve, respectively. Once a thumbtack poked a hole in the middle Parafilm between the LAMP zone and the top paper layer and activated the Parafilm valve, the blue food dye automatically flowed through all hydrophilic channels and was delivered to the three nanosensor detection zones in the top layer in less than 3 seconds *via* the capillary effect, after flipping over the device. As shown in Fig. 2B, the blue color spread evenly through the channels and dyed the detection zones blue without using any pneumatic or other pumps, which confirmed successful reagent delivery.

Moreover, we further tested the reagent loss due to evaporation from the device during the LAMP process at 63 °C for 1 h by weighing the mass changes during the LAMP process using an analytical balance. Fig. 2C shows there was negligible reagent evaporation loss (~7%) from the device at 63 °C for 1 h.

3.2. Integration of LAMP and nano-biosensors on the fully paper-based microfluidic device

Although it is simple to use LAMP to qualitatively detect the occurrence of amplification based on the byproducts from the reactions, it is challenging for LAMP for quantitative analysis.[58,63] Herein, ssDNA probe-functionalized GO nano-biosensors were integrated on μFPAD for specific and quantitative detection of LAMP amplicons. The graphene oxide concentration needs to be optimized because it affects fluorescence quenching and recovery of nanosensors. To optimize the GO concentration, five different concentrations ranging from 0.01 mg ml^{-1} up to 0.05 mg ml^{-1} were evaluated. Different fluorescence intensities of different concentrations of GO before and after recovery are illustrated in Fig. 3. It was observed that low and high GO concentrations exhibited lower recovery. It is probably because too low GO concentrations caused inefficient fluorescence quenching and too high GO concentrations resulted in difficult fluorescence recovery. To choose optimal GO concentrations, not only the fluorescence intensity after recovery but also the net recovered fluorescence intensity (the difference between the fluorescence intensities before and after recovery) was considered. Given higher fluorescence intensity after recovery and higher net recovered fluorescence intensity from 0.03 mg mL^{-1}, the GO concentration of 0.03 mg mL^{-1} was applied for subsequent experiments. In addition, turn-on efficiencies of the GO sensor were calculated for different concentrations of GO. The turn-on efficiencies were from 61% to 82%, and 0.03 mg mL^{-1} of GO presented the highest turn-on efficiency (82%).

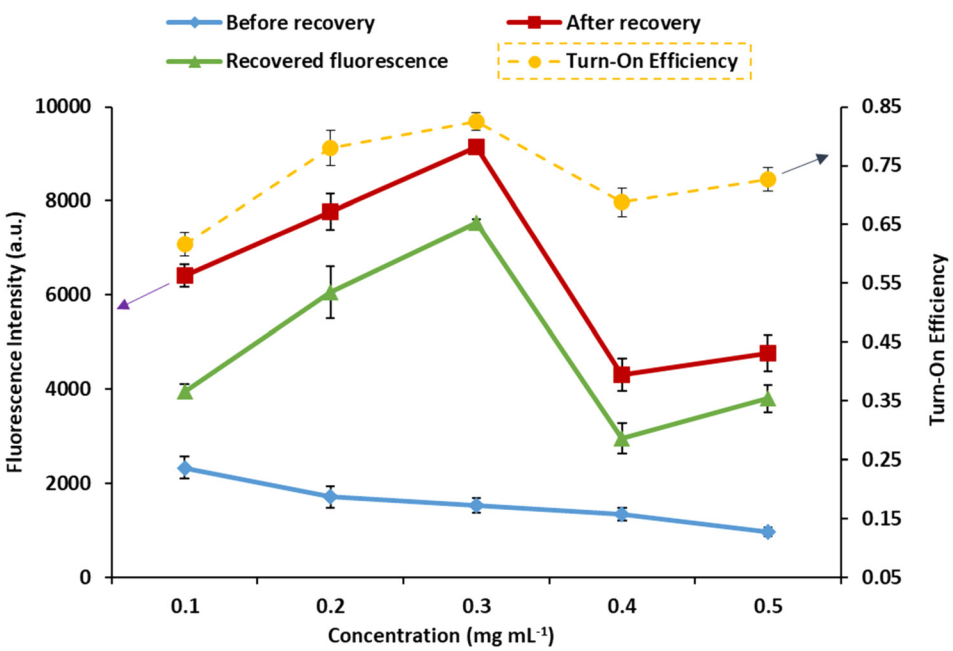

Fig. 3 Optimization of the GO concentrations. Fluorescence intensities of LAMP products before and after recovery, the net recovered fluorescence, and the turn-on efficiency for different concentrations of GO. Error bars represent standard deviations (n = 6).

After optimizing GO concentrations, the μFPAD was used to test *N. meningitides*. After going through on-chip LAMP and nanosensors, Fig. 4A shows on-chip LAMP *N. meningitidis* detection results from fluorescence images before and after fluorescence recovery by keeping one detection zone without the ssDNA probe as negative control (NC) and the other detection zones for *N. meningitidis*. As shown in Fig. 4A(b), the detection zones for *N. meningitidis* detection exhibited strong fluorescence, while no fluorescence was observed in the detection zone for NC. The recovered fluorescence intensity (Fig. 4B) from *N. meningitidis* was about 8-fold higher than that from the negative control. In addition, LAMP products were extracted for the gel electrophoresis test. The LAMP reaction produced a mixture of stem-loop DNA products of different sizes.[64,65] As shown in Fig. 4C, the specific ladder-pattern bands of LAMP products from *N. meningitidis* presented a mixture of DNA amplicons with various sizes due to loop-mediated amplification reactions, which confirmed the successful on-chip LAMP reactions using μFPAD to detect *N. meningitidis*.

3.3. Analytical performance of the μFPAD for quantitative detection

Our paper-based microfluidic nano-biochip can qualitatively detect the targets and present quantitative analysis because of the integrated nano-biosensors. This is one of the significant features of our device because most reported on-chip LAMP methods did not present quantitative analysis.[41,66–68] We evaluated the calibration curve, detection sensitivity, and LOD of our device to detect *N. meningitidis* by testing a series of 10-fold diluted initial template DNA samples (*i.e.*, 6×10^6, 6×10^5, 6×10^4, 6×10^3, 6×10^2, 6×10^1, 6×10^0, and 6×10^{-1} DNA copies per LAMP zone before LAMP amplification) on this microfluidic device after 1 h LAMP amplification reaction. The recovered fluorescence intensities corresponding to different copy numbers of the initial template DNA were achieved from various nano-biosensor detection zones to obtain the calibration curve. As illustrated in Fig. 5, the linear range of the calibration curve is from 6 to 6×10^6 copies per detection zone with the square of the correlation coefficient of 0.9892 (R^2). Based on the 3-fold standard deviations of the mean fluorescence intensities of the negative control, the LOD was achieved to be as low as 6 copies of *N. meningitidis* per detection zone, which was comparable to that of the real-time qPCR.[69,70]

To investigate the specificity of the proposed device for meningitis diagnosis, *N. meningitidis* and *Streptococcus pneumoniae* (*S. pneumoniae*) DNA samples with their corresponding and non-corresponding ssDNA probes were tested because *S. pneumonia* is a rare but serious and life-threatening form of bacterial meningitis. As shown in Fig. 6A, specific ssDNA probes for *N. meningitidis* (N.M.) and *S. pneumoniae* (S.P.) were pre-loaded in the right and left

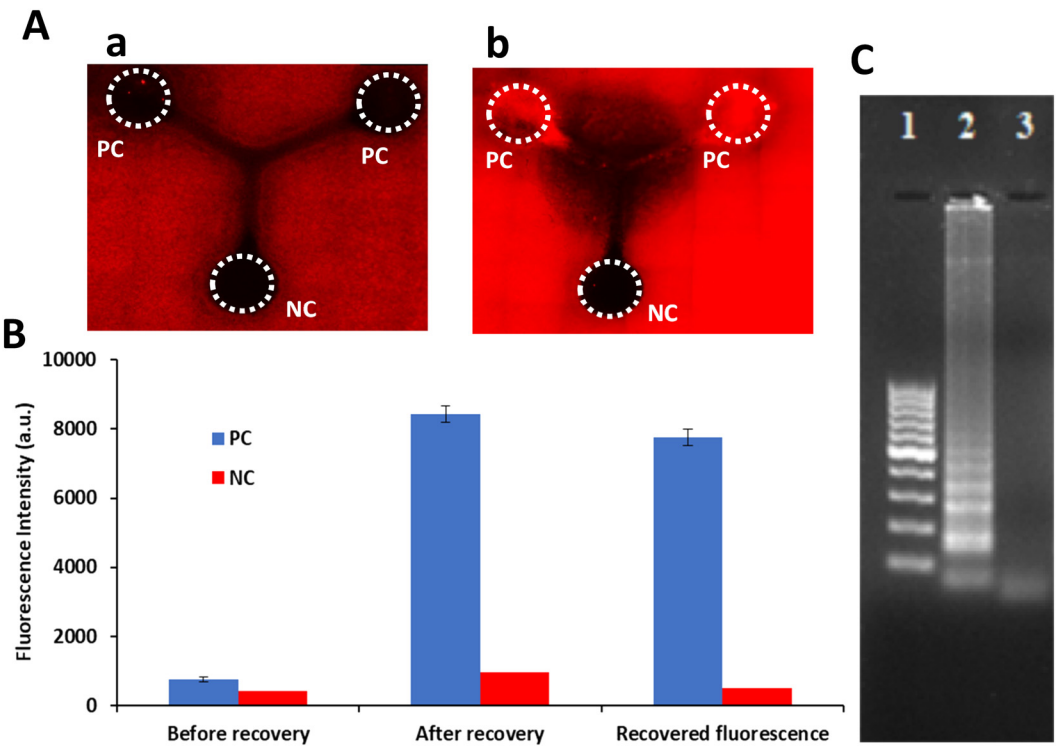

Fig. 4 (A) On-chip LAMP detection of *N. meningitidis* DNA by fluorescence microscopy before fluorescence recovery (a) and after fluorescence recovery (b). Strong fluorescence was observed in positive control detection zones but not in the negative control detection zone. (B) Fluorescent intensity of the different detection zones. (C) Gel electrophoresis analysis of collected LAMP products for a confirmatory test. Lanes 1–3 were 100 bp ladder, the LAMP products from *N. meningitidis*, and the negative control, respectively. The purified DNA template was 6×10^5 copies per LAMP zone.

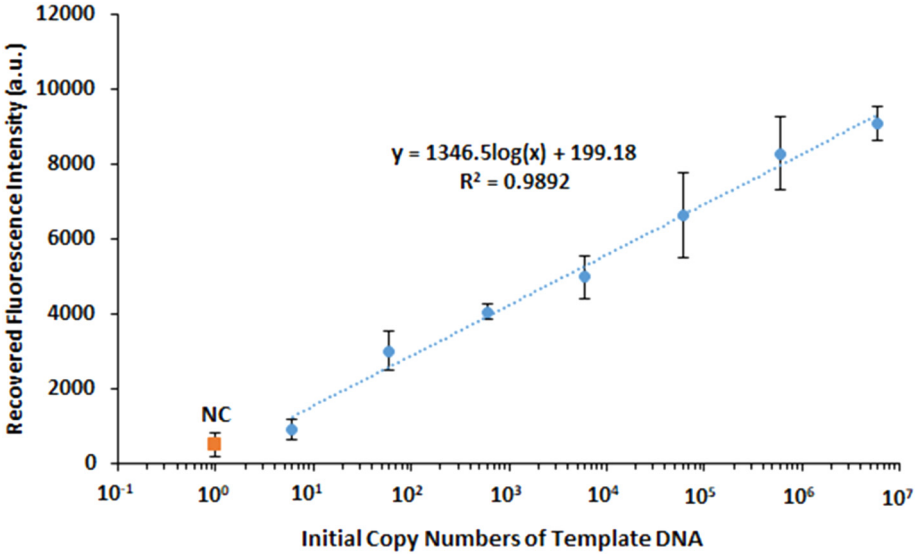

Fig. 5 The linear calibration curve of the net recovered fluorescence intensities *versus* the initial copy number of template DNA (before LAMP amplification) of *N. meningitides*, with the R^2 value of 0.9892. Error bars represent standard deviations (n = 6).

detection zones, respectively. Then, DNA samples of *N. meningitidis* (6×10^5 copies per LAMP zone) were injected into the reaction well for the LAMP reaction. It can be seen from Fig. 6A that only the N.M. ssDNA probe zone that correlated to the corresponding target sample (*i.e.*, N.M. DNA samples) instead of the S.P. probe generated bright fluorescence. When testing *N. meningitidis* DNA samples, the fluorescence intensity of the detection zone with pre-loaded *N. meningitidis* ssDNA probes (*i.e.*, N.M. probe + N.M. DNA sample) from Fig. 6C was about 4-fold higher than the nano-biosensor zone with *S. pneumoniae* ssDNA probes (*i.e.*, S.P. probe + N.M. DNA sample). In addition, using the μFPAD with pre-loaded N.M. probes, we introduced *S. pneumoniae* (6×10^6 copies per LAMP zone) into the device to further test its specificity. As shown in Fig. 6B, after pre-loading the *N. meningitidis* ssDNA probes and injection of the DNA samples of *S. pneumonia* (*i.e.*, N.M. probe + S.P. DNA sample), no noticeable fluorescence was generated. As shown in Fig. 6D, when testing *S. pneumoniae* DNA samples, the fluorescence intensity of the detection zones pre-loaded with *N. meningitidis* ssDNA probes was as dim as that of the negative control. Both specificity tests have confirmed the high specificity of the μFPAD for meningitis detection, mainly contributed by double checkpoints through specific LAMP primers and specific DNA capture probes.

Moreover, multiple pathogens can coexist in many cases of real samples. Multiplexed pathogens detection provides convenience from a single assay and richer information of several pathogens at a time.[37] Therefore, the multiplexing capacity of the proposed μFPAD in multiplexed pathogens detection was further investigated. *N. meningitidis* and *S. pneumoniae* were simultaneously detected using the μFPAD integrated with ssDNA-functionalized GO nano-biosensors. The right and left detection zones were pre-loaded with ssDNA probes of *N. meningitidis* and *S. pneumoniae*, respectively, and the bottom detection zone was used as the negative control. The DNA samples of *N. meningitidis* and *S. pneumoniae* and corresponding primers were injected into the reaction well of the microfluidic device for LAMP reactions and the subsequent nanosensor detection. As shown in Fig. 7, strong fluorescence was produced from the corresponding reaction wells of *N. meningitidis* and *S. pneumoniae* which were much higher than that of the NC. The recovered fluorescence intensities from *N. meningitidis* and *S. pneumoniae* were about 8-fold higher than the negative control. A single device readily achieved multiplexed detection of *N. meningitidis* and *S. pneumonia*. Therefore, the successful multiplexed detection of both *N. meningitidis* and *S. pneumoniae* has demonstrated the tremendous potential of the μFPAD for sensitive and specific detection of various pathogens while leveraging the advantages of high sensitivity from LAMP amplification, high specificity from LAMP and DNA probes, quantitation functionality from nanosensors, and low cost and high portability from the fully paper-based microfluidic device.

To validate our microfluidic device, two different concentrations (60 and 600 DNA copies) of *N. meningitidis* spiked in human whole serum were tested using the proposed μFPAD and the results are listed in Table 2. *N. meningitidis* was not detectable using our device in the human serum samples without spiked *N. meningitidis*. Other spiked samples at concentrations of 60 and 600 DNA copies of *N. meningitidis* showed recovery percentages of 97.2% and 98.5%, respectively. These results are within the acceptable range for the validation of analytical methods,[71] which not only validated the accuracy of our approach but also

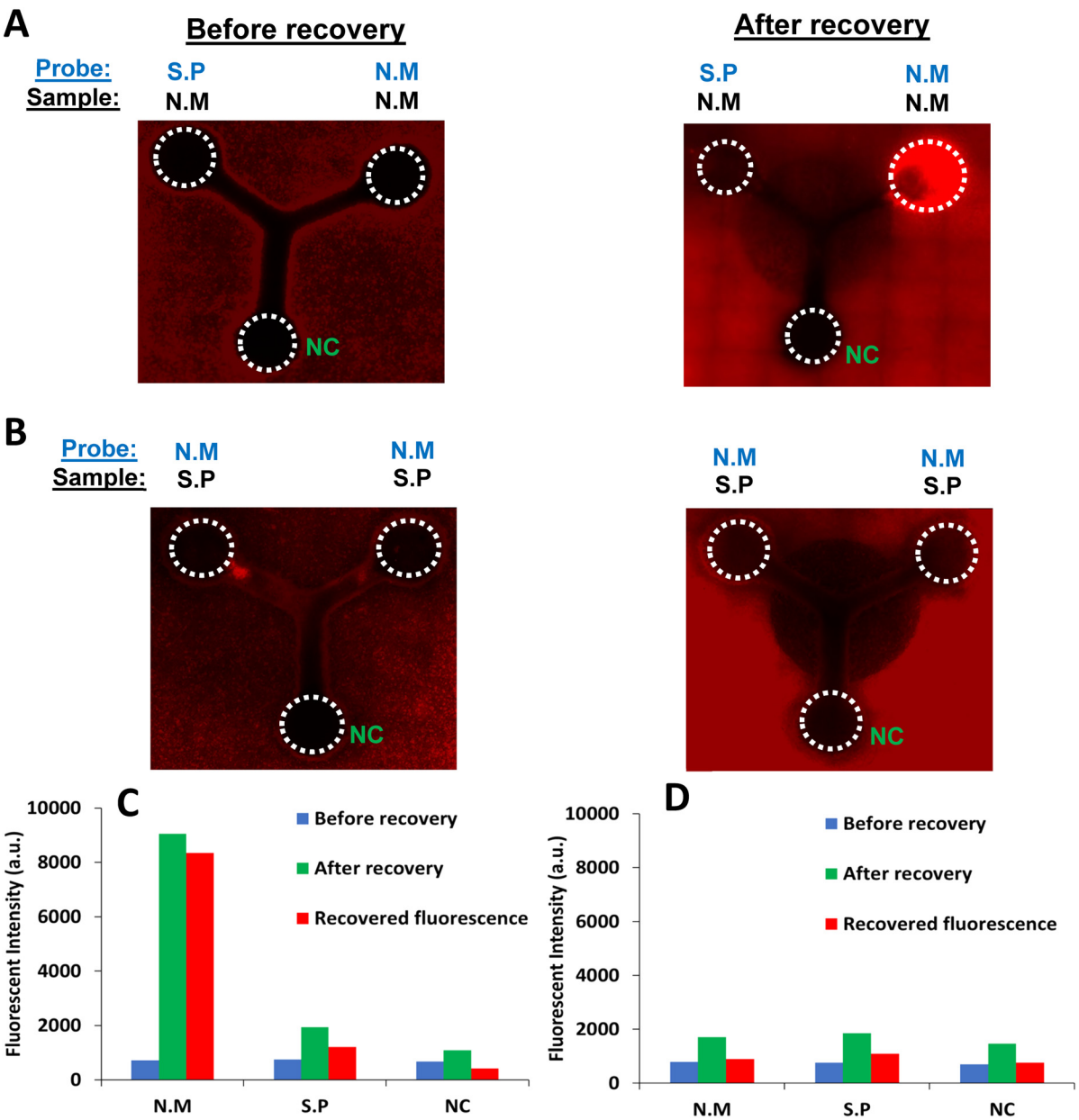

Fig. 6 (A) Fluorescence images of μFPAD before and after recovery for specificity investigation by testing *N. meningitides* (N.M.) samples with their corresponding and non-corresponding ssDNA probes. (B) Fluorescence images of μFPAD before and after recovery for specificity investigation by testing *S. pneumoniae* (S.P.) samples with *N. meningitidis* ssDNA probes. (C) Fluorescence intensities of nano-biosensor zones before and after recovery for specificity investigation by testing *N. meningitidis* samples with its corresponding and non-corresponding ssDNA probes. (D) Fluorescence intensities of nano-biosensor zones before and after recovery for specificity investigation by testing *S. pneumoniae* samples with *N. meningitidis* ssDNA probes.

indicated the robustness of the μFPAD in testing complex human samples.

4. Conclusions

In this study, a simple and low-cost fully paper-based microfluidic device integrated with LAMP, smart one-touch actuation, and ssDNA probe-functionalized GO nano-biosensors for rapid and sensitive quantitative detection of infectious diseases with high specificity. The LOD of 6 DNA copies per reaction zone was achieved in detecting *N. meningitides* in 1 h. This microfluidic approach has the following significant features. (1) Among various chip substrate materials from silicon to paper for microfluidics, this microfluidic device is fully made of paper, making it easy to fabricate and incinerate with low costs. Importantly, this work pioneered the integration of LAMP on a fully paper-based device and, for the first time, achieved LAMP integration on a fully-based microfluidic device without noticeable reagent losses on paper due to evaporation. (2) This device integrates multiple assay steps on a single device

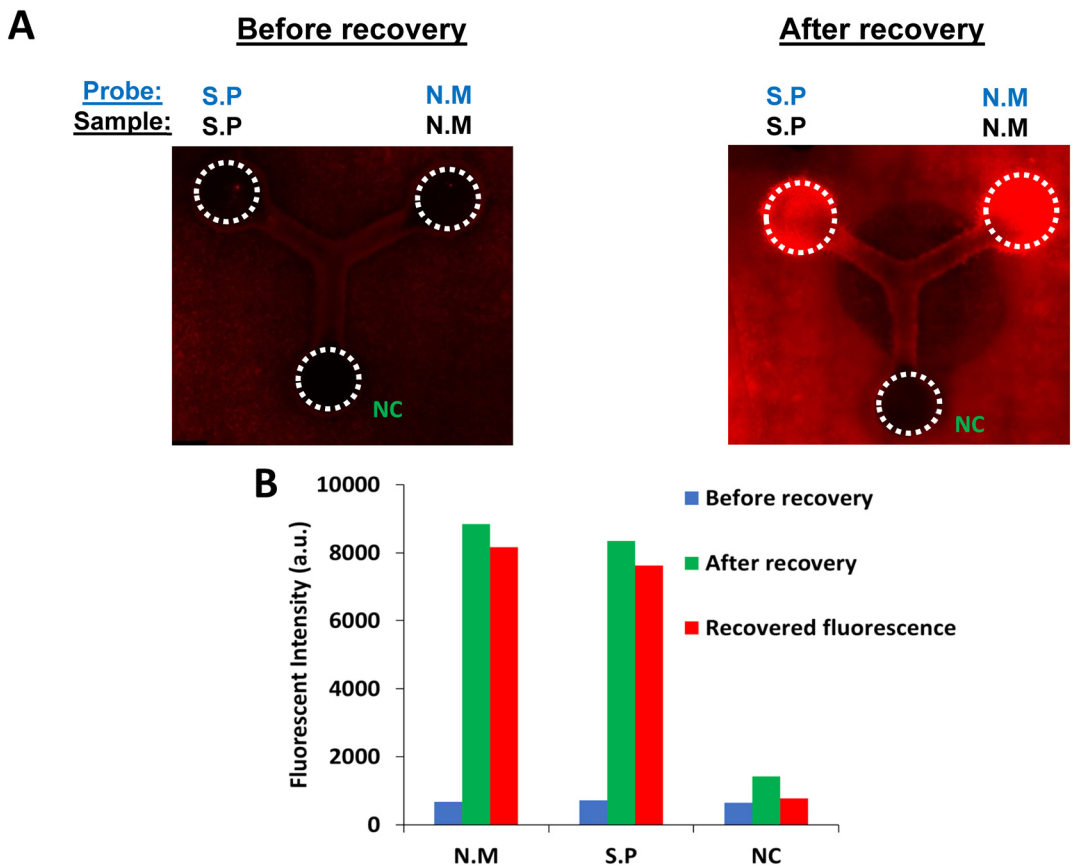

Fig. 7 Multiplexed detection of *N. meningitidis* (N.M.) and *S. pneumoniae* (S.P.). (A) Fluorescence images of the μFPAD integrated with LAMP and ssDNA functionalized GO nano-biosensors for multiplexed detection of *N. meningitidis* and *S. pneumoniae* before and after fluorescence recovery. (B) The corresponding fluorescence intensities of the nano-biosensor detection zones before and after recovery. The purified DNA templates of *N. meningitidis* and *S. pneumoniae* were 6×10^5 copies per LAMP zone.

Table 2 Determination of *N. meningitidis* spiked in human serum samples (n = 4)

Sample	Added *N. meningitidis* (copies/well)	Detected *N. meningitidis* (copies/well)	Recovery (%)
Human serum sample	0	N.D.[a]	—
	60	58.3	97.2 ± 3.8
	600	591.2	98.5 ± 3.1

[a] Not detectable.

from pre-loaded reagents, LAMP, smart one-touch actuation, and nanosensor detection, minimizing contamination due to sample transfer and end user's operation steps while enhancing high portability. The combination of the device with a portable fluorometer or a smartphone camera could further enhance its portability for on-site detection in low-resource settings.[72] (3) The μFPAD offers not only high sensitivity due to the integrated LAMP amplification, which is comparable to the costly conventional method qPCR but also high specificity due to double checkpoints from LAMP and DNA probes. (4) This paper-based microfluidic device offers versatile functions. It is not only capable of qualitative analysis but also quantitative detection, addressing a major problem in LAMP detection. Additionally, the design of the microfluidic device allows easy extraction of on-chip LAMP products for other confirmatory tests such as gel electrophoresis. However, extracted DNA samples were used to demonstrate the proof of concept of the μFPAD for pathogens detection in this work. To minimize off-chip sample preparation steps,[48] a simple on-chip lysis procedure developed recently by our group[18,73] will be integrated into the microfluidic device for instrument-free detection of pathogens in our future work. (5) The demonstrated multiplexed detection of *N. meningitides* and *S. pneumoniae* shows tremendous potential and wide applications of the μFPAD for simultaneous quantitation of various infectious diseases such as on-site detection of COVID-19 caused by SARS-CoV-2.

Conflicts of interest

A provisional patent was filed by XL. Other authors declare no conflicts of interest.

Acknowledgements

We would like to acknowledge the financial support from the National Institute of General Medical Sciences of the NIH (SC2GM105584), the Philadelphia Foundation (Meningitis

Funds), NIH/NIAID (R41AI162477), DOT (CARTEEH), the U.S. NSF (IIP2122712, IIP2052347, IIP1953841, and CHE2216473), and Cancer Prevention and Research Institute of Texas (CPRIT; RP210165). We are also grateful for the financial support for our prior research from the National Institute of Allergy and Infectious Disease of the NIH (R21AI107415), the NIH/NIMHD RCMI Pilot grant (5G12MD007593-22), the NIH BUILDing Scholar Summer Sabbatical Award, NSF (DMR 1827745), the Medical Center of the Americas Foundation (MCA), University of Texas (UT) System for the STARS award, and UTEP for IDR, URI, and MRAP awards.

References

1 A. C. H. de Castro, L. T. Kochi, A. C. R. Moço, R. S. Coimbra, G. C. Oliveira, S. Cuadros-Orellana, J. M. Madurro and A. G. Brito-Madurro, *J. Solid State Electrochem.*, 2018, **22**, 2339–2346.
2 M. Tak, V. Gupta and M. Tomar, *Biosens. Bioelectron.*, 2014, **59**, 200–207.
3 S. K. Dash, M. Sharma, A. Kumar, S. Khare and A. Kumar, *J. Solid State Electrochem.*, 2014, **18**, 2647–2659.
4 J. M. Escolano, B. Díaz-Durán, M. DeMiguel-Ramos, J. Olivares, M. A. Geday and E. Iborra, *Sens. Actuators, B*, 2017, **246**, 591–596.
5 K. Cartwright, D. Jones, E. Kaczmarski, A. Smith, J. Stuart and S. Palmer, *Lancet*, 1991, **338**, 554–557.
6 G. Rai, K. Zachariah, R. Sharma, S. Phadake and K. Belapurkar, *Comp. Immunol., Microbiol. Infect. Dis.*, 2004, **27**, 217–223.
7 G. Rai, K. Zachariah, R. Sharma, S. Phadke and K. Belapurkar, *Comp. Immunol., Microbiol. Infect. Dis.*, 2003, **26**, 261–267.
8 R. C. de Jonge, A. M. van Furth, M. Wassenaar, R. J. Gemke and C. B. Terwee, *BMC Infect. Dis.*, 2010, **10**, 232.
9 S. Negi, S. Grover, S. Rautela, D. Rawat, S. Gupta, S. Khare, S. Lal and A. Rai, *Iran. J. Microbiol.*, 2010, **2**, 73.
10 H. M. Wu, S. M. Cordeiro, B. H. Harcourt, S. C. Maria da Gloria, J. Azevedo, T. Q. Oliveira, M. C. Leite, K. Salgado, M. G. Reis and B. D. Plikaytis, *BMC Infect. Dis.*, 2013, **13**, 26.
11 S. M. de Almeida, L. B. Santana, G. B. Kussen and K. Nogueira, *Curr. HIV Res.*, 2020, **18**, 267–276.
12 I. de Filippis, C. F. de Andrade, N. Caldeira, A. C. de Azevedo and A. E. de Almeida, *Braz. J. Infect. Dis.*, 2016, **20**, 335–341.
13 K. Diallo, M. D. Coulibaly, L. S. Rebbetts, O. B. Harrison, J. Lucidarme, K. Gamougam, Y. K. Tekletsion, A. Bugri, A. Toure and B. Issaka, *PLoS One*, 2018, **13**, e0206453.
14 T. W. Bourke, J. P. McKenna, P. V. Coyle, M. D. Shields and D. J. Fairley, *Lancet Infect. Dis.*, 2015, **15**, 552–558.
15 O. Higgins and T. J. Smith, *J. Mol. Diagn.*, 2020, **22**, 640–651.
16 X. Wang, M. J. Theodore, R. Mair, E. Trujillo-Lopez, M. du Plessis, N. Wolter, A. L. Baughman, C. Hatcher, J. Vuong and L. Lott, *J. Clin. Microbiol.*, 2012, **50**, 702–708.
17 N. Bhatt, N. Khan, S. K. Dash, S. Khare and A. Kumar, *Indian J. Biochem. Biophys.*, 2014, **51**, 211–214.
18 M. Dou, S. T. Sanjay, D. C. Dominguez, P. Liu, F. Xu and X. Li, *Biosens. Bioelectron.*, 2017, **87**, 865–873.
19 O. Higgins, E. Clancy, M. Cormican, T. Boo, R. Cunney and T. Smith, *Int. J. Mol. Sci.*, 2018, **19**, 524.
20 M. Seki, P. E. Kilgore, E. J. Kim, M. Ohnishi, S. Hayakawa and D. W. Kim, *Front. Pediatr.*, 2018, **6**, 57.
21 M. Dou, D. C. Dominguez, X. Li, J. Sanchez and G. Scott, *Anal. Chem.*, 2014, **86**, 7978–7986.
22 M. Dou, N. Macias, F. Shen, J. D. Bard, D. C. Domínguez and X. Li, *EClinicalMedicine*, 2019, **8**, 72–77.
23 G. Fu, Y. Zhu, K. Xu, W. Wang, R. Hou and X. Li, *Anal. Chem.*, 2019, **91**, 13290–13296.
24 S. T. Sanjay, W. Zhou, M. Dou, H. Tavakoli, L. Ma, F. Xu and X. Li, *Adv. Drug Delivery Rev.*, 2018, **128**, 3–28.
25 H. Tavakoli, W. Zhou, L. Ma, S. Perez, A. Ibarra, F. Xu, S. Zhan and X. Li, *TrAC, Trends Anal. Chem.*, 2019, **117**, 13–26.
26 X. Wei, W. Zhou, S. T. Sanjay, J. Zhang, Q. Jin, F. Xu, D. C. Dominguez and X. Li, *Anal. Chem.*, 2018, **90**, 9888–9896.
27 W. Zhou, G. Fu and X. Li, *Anal. Chem.*, 2021, **93**, 7754–7762.
28 L. Ma, Y. Abugalyon and X. Li, *Anal. Bioanal. Chem.*, 2021, 1–9.
29 M. Lv, W. Zhou, H. Tavakoli, C. Bautista, J. Xia, Z. Wang and X. Li, *Biosens. Bioelectron.*, 2021, **176**, 112947.
30 K. Mattern, J. W. von Trotha, P. Erfle, R. W. Köster and A. Dietzel, *Commun. Biol.*, 2020, **3**, 1–6.
31 F. Yang, A. Carmona, K. Stojkova, E. I. G. Huitron, A. Goddi, A. Bhushan, R. N. Cohen and E. M. Brey, *Lab Chip*, 2021, **21**, 435–446.
32 W. Zhou, M. Feng, A. Valadez and X. Li, *Anal. Chem.*, 2020, **92**, 7045–7053.
33 K. S. Prasad, X. Cao, N. Gao, Q. Jin, S. T. Sanjay, G. Henao-Pabon and X. Li, *Sens. Actuators, B*, 2020, **305**, 127516.
34 W. Zhou, H. Tavakoli, L. Ma, C. Bautista and X. Li, in *Multidisciplinary Microfluidic and Nanofluidic Lab-on-a-chip*, Elsevier, 2022, pp. 325–360.
35 H. Tavakoli, W. Zhou, L. Ma, Q. Guo and X. Li, *Nanotechnology for Microfluidics*, 2020, pp. 177–209.
36 S. X. Fu, P. Zuo and B. C. Ye, *Biotechnol. J.*, 2021, **16**, 2000126.
37 P. Zuo, X. Li, D. C. Dominguez and B.-C. Ye, *Lab Chip*, 2013, **13**, 3921–3928.
38 X. Y. Liu, M. Mwangi, X. J. Li, M. O'Brien and G. M. Whitesides, *Lab Chip*, 2011, **11**, 2189–2196.
39 L. Cao, X. Guo, P. Mao, Y. Ren, Z. Li, M. You, J. Hu, M. Tian, C. Yao and F. Li, *ACS Sens.*, 2021, **6**, 3564–3574.
40 P. Chen, C. Chen, Y. Liu, W. Du, X. Feng and B.-F. Liu, *Sens. Actuators, B*, 2019, **283**, 472–477.
41 C. Xie, S. Chen, L. Zhang, X. He, Y. Ma, H. Wu, B. Zou and G. Zhou, *Anal. Bioanal. Chem.*, 2021, **413**, 2923–2931.
42 S.-C. Chen, C.-C. Liu, Y.-N. Wang, L.-M. Fu and S.-H. Shih, *Chem. Eng. J.*, 2018, **334**, 1828–1834.
43 Z. Shi, N. Dong, X. Lai, H. Yu and D. Li, *21st International Conference on Solid-State Sensors, Actuators and Microsystems (Transducers)*, 2021, pp. 976–979.
44 B. Pang, K. Fu, Y. Liu, X. Ding, J. Hu, W. Wu, K. Xu, X. Song, J. Wang and Y. Mu, *Anal. Chim. Acta*, 2018, **1040**, 81–89.
45 F. Figueredo, F. Stolowicz, A. Vojnov, W. K. Coltro, L. Larocca, C. Carrillo and E. Cortón, *PLoS Neglected Trop. Dis.*, 2021, **15**, e0009406.

46 H. Wang, Z. Ma, J. Qin, Z. Shen, Q. Liu, X. Chen, H. Wang, Z. An, W. Liu and M. Li, *Biosens. Bioelectron.*, 2019, **126**, 373–380.

47 W. Witkowska McConnell, C. Davis, S. R. Sabir, A. Garrett, A. Bradley-Stewart, P. Jajesniak, J. Reboud, G. Xu, Z. Yang and R. Gunson, *Nat. Commun.*, 2021, **12**, 1–8.

48 K. Kaarj, P. Akarapipad and J.-Y. Yoon, *Sci. Rep.*, 2018, **8**, 12438.

49 Y. Seok, H.-A. Joung, J.-Y. Byun, H.-S. Jeon, S. J. Shin, S. Kim, Y.-B. Shin, H. S. Han and M.-G. Kim, *Theranostics*, 2017, **7**, 2220.

50 I. Hongwarittorrn, N. Chaichanawongsaroj and W. Laiwattanapaisal, *Talanta*, 2017, **175**, 135–142.

51 I. Choopara, A. Suea-Ngam, Y. Teethaisong, P. D. Howes, M. Schmelcher, A. Leelahavanichkul, S. Thunyaharn, D. Wongsawaeng, A. J. DeMello and D. Dean, *ACS Sens.*, 2021, **6**, 742–751.

52 W. Zhou, M. Dou, S. S. Timilsina, F. Xu and X. Li, *Lab Chip*, 2021, **21**, 2658–2683.

53 M. Dou, S. T. Sanjay, M. Benhabib, F. Xu and X. Li, *Talanta*, 2015, **145**, 43–54.

54 S. T. Sanjay, G. Fu, M. Dou, F. Xu, R. Liu, H. Qi and X. Li, *Analyst*, 2015, **140**, 7062–7081.

55 A. Suea-Ngam, I. Choopara, S. Li, M. Schmelcher, N. Somboonna, P. D. Howes and A. J. deMello, *Adv. Healthcare Mater.*, 2021, **10**, 2001755.

56 M. Dou, S. T. Sanjay, D. C. Dominguez, S. Zhan and X. Li, *Chem. Commun.*, 2017, **53**, 10886–10889.

57 M. Dou, J. M. García, S. Zhan and X. Li, *Chem. Commun.*, 2016, **52**, 3470–3473.

58 M. Dou, J. Sanchez, H. Tavakoli, J. E. Gonzalez, J. Sun, J. Dien Bard and X. Li, *Anal. Chim. Acta*, 2019, **1065**, 71–78.

59 Y. Gao, J. Tian, X. Zhang, B. Qiao, Y. Cao, X. Wang and Q. Wu, *Analyst*, 2020, **145**, 1190–1194.

60 S. PK, C. Bathula, C. KN and M. Das, *J. Agric. Food Chem.*, 2020, **68**, 3656–3662.

61 B. Shin, J.-S. Park, H.-S. Chun, S. Yoon, W.-K. Kim and J. Lee, *Anal. Bioanal. Chem.*, 2020, **412**, 233–242.

62 J. Zhou, R. Ai, J. Weng, L. Li, C. Zhou, A. Ma, L. Fu and Y. Wang, *Microchem. J.*, 2020, **158**, 105171.

63 M. Dou, S. T. Sanjay, D. C. Dominguez, S. Zhan and X. Li, *Chem. Commun.*, 2017, **53**, 10886–10889.

64 N. Tomita, Y. Mori, H. Kanda and T. Notomi, *Nat. Protoc.*, 2008, **3**, 877.

65 T. C. Lin, W. V. Hsiao, S. J. Han, S. J. Joung and J. C. Shiao, *Aquat. Conserv.: Mar. Freshw. Ecosyst.*, 2021, **31**, 2193–2203.

66 V. Varsha, S. Aishwarya, S. Murchana, G. Naveen, M. Ramya and P. Rathinasabapathi, *J. Microbiol. Methods*, 2020, **174**, 105962.

67 D. Liu, Y. Zhu, N. Li, Y. Lu, J. Cheng and Y. Xu, *Sens. Actuators, B*, 2020, **310**, 127834.

68 J. Jawla, R. R. Kumar, S. Mendiratta, R. Agarwal, S. Kumari, V. Saxena, D. Kumar, P. Singh, N. Boby and P. Rana, *Anal. Chim. Acta*, 2021, **1150**, 338220.

69 G. M. Abdeldaim, K. Strålin, J. Korsgaard, J. Blomberg, C. Welinder-Olsson and B. Herrmann, *BMC Microbiol.*, 2010, **10**, 310.

70 N. Chiba, S. Y. Murayama, M. Morozumi, E. Nakayama, T. Okada, S. Iwata, K. Sunakawa and K. Ubukata, *J. Infect. Chemother.*, 2009, **15**, 92–98.

71 S. Zhou, W. Zheng, Z. Chen, D. Tu, Y. Liu, E. Ma, R. Li, H. Zhu, M. Huang and X. Chen, *Am. Ethnol.*, 2014, **126**, 12706–12710.

72 X. Xu, X. Wang, J. Hu, Y. Gong, L. Wang, W. Zhou, X. Li and F. Xu, *Electrophoresis*, 2019, **40**, 914–921.

73 M. Dou, J. Sanchez, H. Tavakoli, J. E. Gonzalez, J. Sun, J. D. Bard and X. Li, *Anal. Chim. Acta*, 2019, **1065**, 71–78.